# INSTITUTE FOR FUSION STUDIES

DOE/ET-53088-497 IFSR #497

## Nonlinear Dynamic Models Displaying Temporal Features of Sawtooth Oscillations[†]

A. THYAGARAJA[*] and F.A. HAAS[*]
Institute for Fusion Studies
The University of Texas at Austin
Austin, Texas 78712

April 1991

[†]Presented at the 1991 International Sherwood Fusion Theory Conference, April 22-24, 1991, Seattle, Washington

[*]permanent address: UKAEA/EURATOM Fusion Association, Culham Laboratory, Abingdon, Oxon OX14 3DB, UNITED KINGDOM

# THE UNIVERSITY OF TEXAS


# AUSTIN

# Nonlinear Dynamic Models Displaying Temporal Features of Sawtooth Oscillations

A. Thyagaraja* and F.A. Haas

UKAEA/EURATOM Fusion Association, Culham Lab.
Abingdon, Oxon. OX14 3DB, UK.

## Abstract

There is at present no completely satisfactory theory of sawteeth in tokamaks. Although the simulations of Denton et al (Phys. Rev. Letts. **56**, 2477, 1986) and Aydemir et al (Phys. Fluids **B**1, 744, 1989) capture some of the periodicity properties, they do not show the partial reconnection currently observed in experiments. It would seem useful to construct the simplest possible nonlinear dynamical model to illustrate some of the temporal features of sawteeth. To this end, we introduce the variables $y(t)$ and $x(t)$, which represent the internal energy and the magnetic turbulence amplitude respectively. These are assumed to be governed by the pair of nonlinear differential equations

$$\tau_s \frac{dy}{dt} = (1 - \lambda x^2) + f_y(t) \qquad (1)$$

$$\tau_s \frac{dx}{dt} = \lambda x(y-1)\phi(x,\lambda) + f_x(t) \qquad (2)$$

where $\tau_s$ is a typical "ramp" time scale and $\lambda$ is a large parameter. $f_y(t)$ and $f_x(t)$ are Langevin-type "noise" functions. Two

simple heuristic choices have been tried for the function $\phi$, namely $\phi = 1$ and $\phi = \frac{2\lambda x^2}{1+\lambda x^2}$. The Eq.(1) represents energy balance with confinement degradation in response to turbulence, while Eq.(2) represents the dynamic relationship between the plasma internal energy and magnetic turbulence. Both analytic and numerical solutions show $y(t)$ to have the characteristic sawtooth waveform for large $\lambda$ with the sawtooth period $\tau_{period} = 2\tau_s(1 + \log\lambda/\lambda)$ and $\tau_{crash} = \tau_{period} \log\lambda/\lambda$. The variable $x(t)$ is small during the ramp but behaves in a $\delta$-function-like manner during the crash. The effects of noise are investigated. The second model is found to be more robust to noise and has a physically more reasonable behaviour for $x(t)$ than the $\phi \equiv 1$ model. Both models suggest the possibility that the interplay of transport and dynamics is capable of yielding the gross temporal properties of sawteeth. Comparison with more elaborate numerical simulations suggests that the tentative interpretation of the dynamical variables may be a reasonable one.

* Currently visiting the Institute of Fusion Studies, University of Texas at Austin, Austin, Texas 78712.

## I. Introduction & Motivation

- Sawtooth oscillations in tokamaks exhibit quite complex spatial and temporal behaviour. At the present time there is no fully satisfactory theory which accounts for the wealth of experimental observations relating to this phenomenon.

- The purpose of this contribution is to construct very simple dynamical models which may throw some light on the nature of sawteeth. There is at present no direct derivation of the equations of the model from more complete physics. There are indications from some numerical simulations of sawteeth that realistic models may indeed behave in some respects in the manner suggested by the simpler models.

- Since we are concerned with temporal dynamical features, the periodicity in time suggests that models could effectively be restricted to two degrees of freedom. Indeed, more degrees of freedom generically lead to chaotic motions which are actually not seen in experiment in the gross scales typical of sawteeth.

- In view of the above, we consider a variable $y(t)$, which is to be regarded as a normalized measure of central temperature. We also introduce another variable $x(t)$ which it is convenient to think of as a measure of magnetic turbulence amplitude within the $q < 1$ zone.

- In the first instance, we shall consider an autonomous pair of nonlinear differential equations Eq.(1) and Eq.(2) with $f_y(t)$ and $f_x(t)$ set identically to zero. The first equation is the analogue of the energy equation with the second term $\lambda x^2$ representing a turbulence-driven loss process. The second equation represents the dynamical coupling between internal energy /temperature and the magnetic turbulence. The time-scale $\tau_s$ measures the scale of variation of $y(t)$ when the turbulent losses are small. The second equation exhibits growth or decay of turbulence when a temperature threshold (the critical value of $y$ is normalized to unity without loss of generality) is crossed.

## II. Analysis of the simple model

- We now consider the analytic treatment of Eqs.(1),(2) in the simpler case when the function $\phi$ is taken to be unity.

- It is convenient to introduce the variables, $Z \equiv \lambda^{\frac{1}{2}}(y-1)$, $v \equiv 2\log(\lambda x)$, and $u \equiv \lambda^{\frac{1}{2}}\frac{t}{\tau_s}$. It is useful to remember that $x(t) > 0$ for all $t$ provided it is so at $t = 0$.

- Since the unbounded elementary solution, $x \equiv 0, y = y(0)+\frac{t}{\tau_s}$, is in fact unstable for any value of $y(0)$ as $t \to \infty$, the variable $v$ is clearly always well-defined.

- The equations now take the form:

$$\frac{dZ}{du} = 1 - \exp v \tag{3}$$

$$\frac{dv}{du} = 2Z \tag{4}$$

This system is equivalent to the second-order non-linear equation,

$$\frac{1}{2}\frac{d^2v}{du^2} = 1 - \exp v \tag{5}$$

- This must be solved subject to the initial conditions, $\frac{dv}{du} = 0$, $v = -k$ at $u = 0$, where $k$ is positive.

- This equation admits the first integral,

$$\frac{1}{4}(\frac{dv}{du})^2 = v - \exp v + k + \exp(-k) \tag{6}$$

- The RHS of Eq.(6) increases with $v$ in the interval $-k \leq v \leq 0$ and decreases with $v$ for $v > 0$. At $v = 0$, it attains its positive maximum value of $(k-1) + \exp(-k)$. Evidently, it has a unique positive zero which we denote by $v_+(k)$.

- From Eq.(6) we see that $v(u;k)$ is a periodic function of u for every $k > 0$, which can be obtained by inverting the integral,

$$2u = \int_{-k}^{v} \frac{dw}{(k + \exp(-k) + w - \exp w)^{\frac{1}{2}}}. \tag{7}$$

- This equation defines a new class of transcendental periodic functions of the real variable $u$ and the positive parameter $k$, which are not apparently reducible to elementary functions, elliptic functions or hyperelliptic functions.

- The period in physical units used in Eqs.(1) and(2) is given by the relation,

$$\tau_{period} = \frac{\tau_s}{\lambda^{\frac{1}{2}}} \int_{-k}^{v_+(k)} \frac{dw}{(k + \exp(-k) + w - \exp w)^{\frac{1}{2}}}, \qquad (8)$$

where, $v_+(k) > 0$ is defined as the positive root of the equation,

$$\exp v_+ - v_+ = k + \exp(-k). \qquad (9)$$

- **The results become much simpler when we assume $\lambda \gg 1$. In this case, we normalize the solution so that the maximum** value of $y(t)$ is normalized to 2 (ie $Z_{max} = \lambda^{\frac{1}{2}}$). Thus $k = \lambda$ and we find that as $u$ varies between $-\lambda^{\frac{1}{2}}$ to $\lambda^{\frac{1}{2}}$, $v$ remains sufficiently negative to imply that $Z$ is linear in $u$.

- The maximum of $Z$ corresponds to $v = 0$. It is easily seen that when $v > 0$, $Z$ 'crashes' relatively rapidly to zero. At this point, $x^2$ attains its maximum value. In fact, we find that $x^2_{max} \approx \{1 + \frac{\log \lambda}{\lambda}\}$, confirming that the crash is indeed associated with large amplitude turbulence.

- The period is readily obtained by an elementary asymptotic analysis (see Haas & Thyagaraja,1990):

$$\tau_{period} = 2\tau_s\{1 + \frac{\log \lambda}{\lambda}\} \tag{10}$$

- The parameter $\lambda$ relates the crash time-scale to the period as follows:

$$\frac{\tau_{crash}}{\tau_{period}} = \frac{\log \lambda}{\lambda} \tag{11}$$

From the preceding equations it is clear that the physical parameters $\tau_{period}$ and $\tau_{crash}$ may be used to fix the values of $\tau_s$ and $\lambda$ which completely characterise the model assuming the normalisation conventions.

## III. Numerical Results: simple model

- The model has been solved numerically. Fig. 1 shows the plots of $y(t)$ and $X(t) = x^2(t)$ for $\tau_s = 8$ msec and $\lambda = 300$. The sawtooth period estimated is 16.3 msec whilst the 'crash' time is of order 300 microsecs.

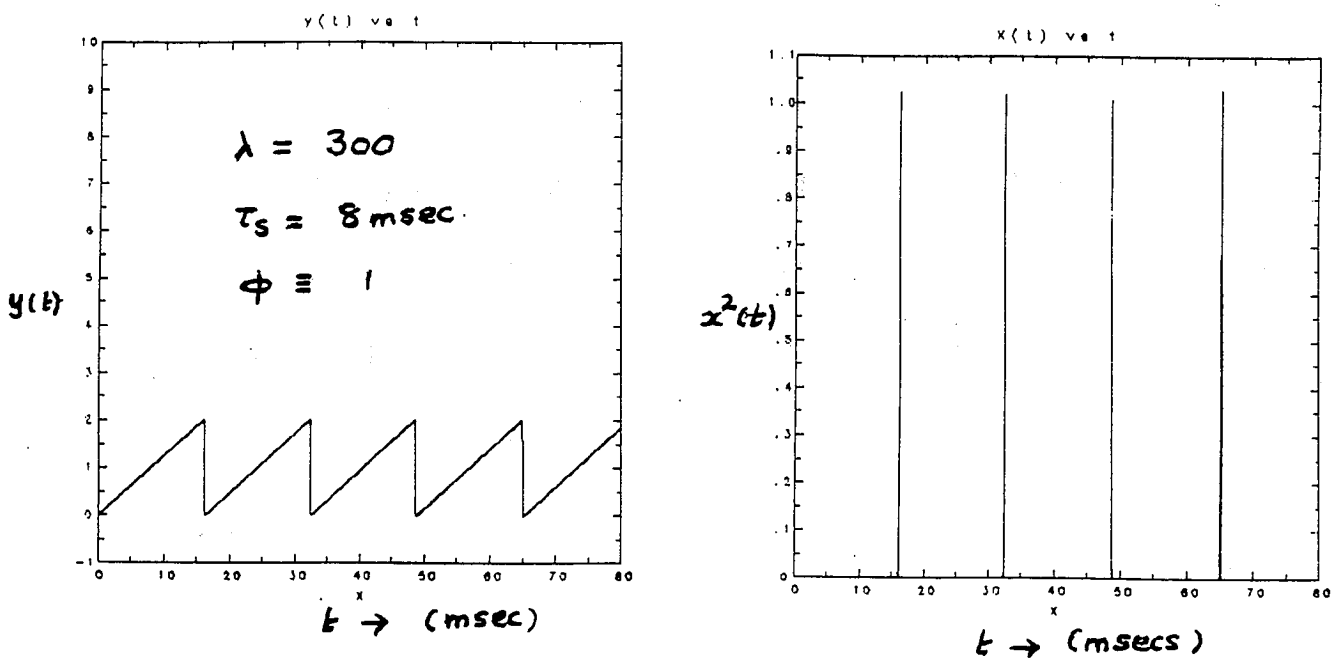


**Fig.1 Simple Model: Unperturbed Solutions**

The numerical values are in good agreement with the analytic theory. The very sharp spikes in $X(t)$ clearly show that the 'turbulence' is only significant during the crash. The time-

step $\Delta t$ was chosen to be 0.1 microsec; the solutions are in fact grid independent.

- It is easily shown from the equations of motion that external perturbations $f_y(t)$ have little or no influence on the basic dynamics discussed. While it is in principle possible to discuss the issue of linear stability of the periodic solution analytically , it is simpler to directly verify this numerically.

- Thus we have solved the equations of motion Eqs.(1),(2), taking $f_x, f_y$ to be simple harmonic forms $f\cos\omega t, g\sin\omega t$. The non- dimensional amplitudes were varied over a wide range as were the frequencies $\omega$. Unless $f_y/\omega\tau_s \simeq 1$, the behaviour relative to such perturbations is uninteresting. Fig.2 shows the effect of a relatively small $f_x = 10^{-6}$, and $\omega\tau_s = 20$ on the system. Clearly the period is substantially reduced as is the amplitude.

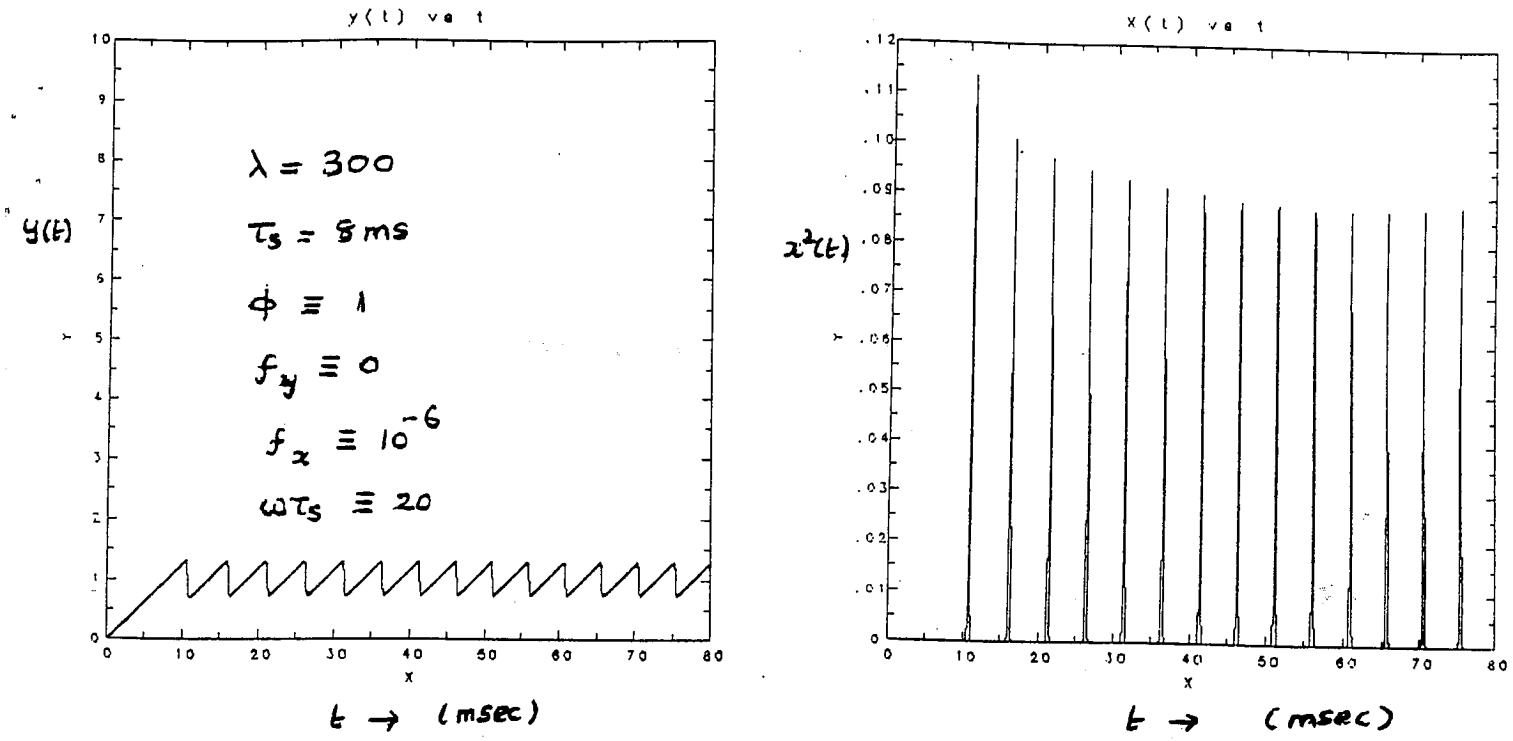


**Fig.2 Simple Model: Perturbed Solutions**

- This behaviour continues until the parameter $\frac{f_x}{\omega\tau_s} \simeq 10^{-1}$, when the solution drastically changes character; the 'saw-toothing' is completely stabilized. For certain ranges of $f_x$ and $\omega\tau_s$ the solution of the system makes a transition to 'chaos'. Fig.3 gives an example of this type of 'aperiodic' behaviour.

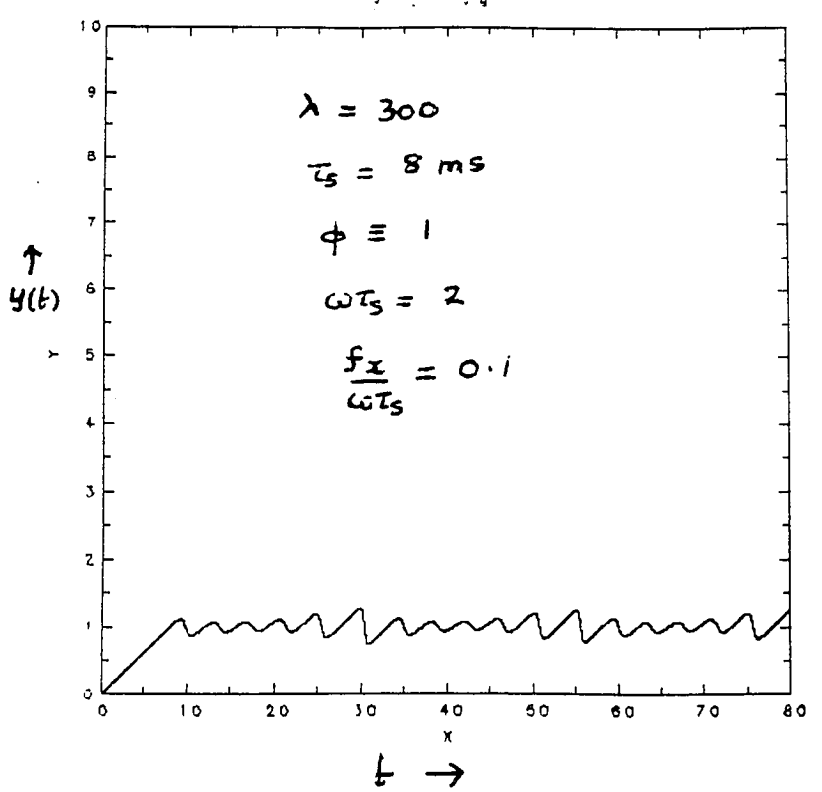


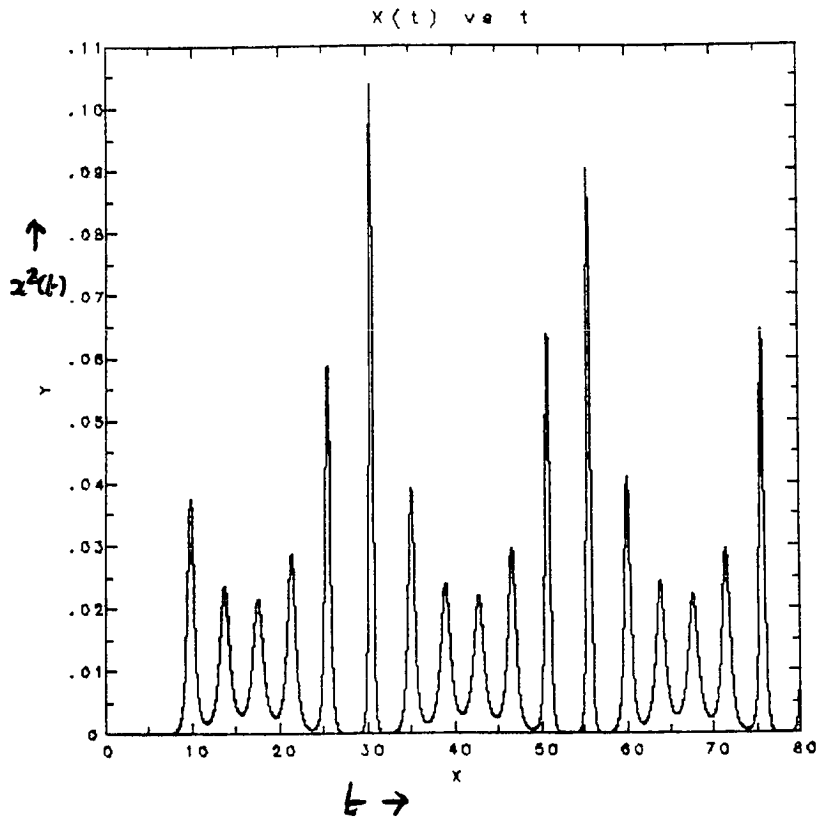


**Fig.3 Simple Model: Chaotic Solutions**

## IV. Improvements to the simple model

- The simple model shows that the sawtooth wave form in $y(t)$ can be associated with a two-degree of freedom, autonomous dynamical system with only quadratic nonlinearities. It appears to be the **simplest** system of its kind. The crash and periodic times are related to the large non-dimensional parameter and the turbulence level behaves in a 'spikey' manner.

- Although the numerical simulations show that the dynamic behaviour is not qualitatively different for the non-autonomous cases when external perturbations are introduced, the amplitude and period are quantitatively altered, especially by forces applied to Eq.(2) for the turbulence amplitude.

- Closely related to this sensitivity is the fact that the system has a symmetry about $y = 1$. Thus the effective growth rate of $x$, $\lambda(y-1)/\tau_s$ for positive $y-1$, is equal and opposite to the decay rate $\lambda(1-y)/\tau_s$ (when $y-1$ is negative but has the same absolute value). This symmetry in the model is of

course a spurious result of its simplicity. Indeed, this implies that when $y = 1$, the value of $x$ must be chosen to be $\exp(-\lambda)$, which can be an unphysically tiny number when $\lambda$ is large.

- These defects are readily removed without sacrificing the basic simplicity. Thus, we set $\phi \equiv \frac{2\lambda x^2}{1+\lambda x^2}$ in Eq.(2). This choice ensures that at the maximum of $y$ when $\lambda x^2 = 1$, the crash behaviour is virtually unaffected. However, during the decay phase, as $x$ decreases, it does not decay at the rate of the simple model, but in an effectively nonlinear way. Thus, the decay is actually algebraic like an inverse power of $t$ for $y < 1$. This implies that in *this* more complicated model, the values of $x^2$ *do not decrease to unphysically small values.*

- While it is not obvious, this modified model is also remarkably stable to external perturbations as will be demonstrated by the numerical simulations presented below.

## V. Analytics of the improved model

- In contrast to the simple model, it is remarkable that this apparently more complicated model can be exactly integrated (in the autonomous case) in terms of elliptic integrals. It is convenient to introduce the variables, $w = y - 1$ and $\theta = \frac{t}{\tau_s}$. Equations of motion in the autonomous case are transformed into,

$$\frac{dw}{d\theta} = 1 - \lambda x^2 \tag{12}$$

$$\frac{dx}{d\theta} = \lambda w x(\frac{2\lambda x^2}{1+\lambda x^2}) \tag{13}$$

- These equations admit the first integral,

$$w^2 = C - \frac{1}{2\lambda^2 x^2} - \frac{x^2}{2} \tag{14}$$

where the constant of integration $C$ evaluates to $C = 1 + \frac{1}{\lambda}$ if we choose the normalisation, $w_{max} = 1$ when $x^2 = \frac{1}{\lambda}$.

- It immediately follows that $x^2$ oscillates periodically in $\theta$ be-

tween the two positive roots of the bi-quadratic,

$$x^4 - 2(1 + \frac{1}{\lambda})x^2 + \frac{1}{\lambda} = 0 \tag{15}$$

Thus, $b^2 \leq x^2 \leq a^2$ where,

$$b^2 = (1 + \frac{1}{\lambda}) - \left[(1 + \frac{1}{\lambda})^2 - \frac{1}{\lambda^2}\right]^{\frac{1}{2}} \tag{16}$$

$$a^2 = (1 + \frac{1}{\lambda}) + \left[(1 + \frac{1}{\lambda})^2 - \frac{1}{\lambda^2}\right]^{\frac{1}{2}} \tag{17}$$

It is obvious that for large $\lambda$, $x_{min} \simeq \frac{1}{\sqrt{2}\lambda}$ and $x_{max} \simeq \sqrt{2(1 + \frac{1}{\lambda})}$. This proves that in this model, the variable $x$ cannot take unphysically small values during the 'ramp' phase. Clearly at the crash, the turbulence level must be large (in relative terms).

- Substituting for $w$ from Eq.(14) into Eq.(13) gives a first order nonlinear equation for $x$ as a function of $\theta$. This is readily integrated in terms of elliptic integrals.

- It is convenient to parametrise the results as follows:

$$m = 1 - \frac{b^2}{a^2} \tag{18}$$

$$\sin^2 \Phi = \frac{1}{m}(1 - \frac{b^2}{x^2}) \tag{19}$$

$$\theta = E(\Phi \mid m) + \frac{F(\Phi \mid m)}{2\lambda} \tag{20}$$

where $F(\Phi \mid m)$ and $E(\Phi \mid m)$ denote the incomplete elliptic integrals of the first and second kind respectively.

- Equivalently, defining the new variable ('elliptic angle') $\varpi$ by $\mathrm{sn}(\varpi \mid m) = \sin \Phi$ we obtain,

$$\frac{x}{b} = \frac{1}{\sqrt{1 - m\mathrm{sn}^2 \varpi}} \tag{21}$$

$$\frac{t}{\tau_s} = \left(\frac{E(m)}{K(m)} + \frac{1}{2\lambda}\right) \varpi + \frac{\Theta'(\varpi)}{\Theta(\varpi)} \tag{22}$$

- In Eq.(22) $\Theta(\varpi)$ is Jacobi's theta function (cf. Whittaker & Watson, p. 479), and $K(m), E(m)$ are the **complete** elliptic

integrals of the first and second kind respectively.

- Bearing in mind that $\Theta$ is an even periodic function and $\mathrm{sn}(\varpi \mid m) = 1$ when $\varpi = K(m)$, the above solution implies that $\tau_{period}$ is given by the relation,

$$\tau_{period} = 2\tau_s(E(m) + \frac{K(m)}{2\lambda}) \tag{23}$$

- It is readily deduced that for large $\lambda$, we must have asymptotically,

$$\tau_{period} = 2\tau_s(1 + \frac{\log\lambda}{2\lambda}) \tag{24}$$

$$\tau_{crash} = 2\tau_s\frac{\log\lambda}{2\lambda} \tag{25}$$

This completes the analytic theory related to the improved model. While it is possible in principle to discuss the linear stability of the solutions to small perturbations analytically, it is a very difficult task. Calculations of the solutions when external perturbations are present are best carried out numerically (as with the simpler model).

## VI. Extended model: numerics

- Fig. 4 shows the numerical solution of Equations (1) and (2) with $\phi = \frac{2\lambda x^2}{1+\lambda x^2}$ for the same values of $\tau_s$(= 8msecs) and $\lambda$(= 300) as for Fig. 1.

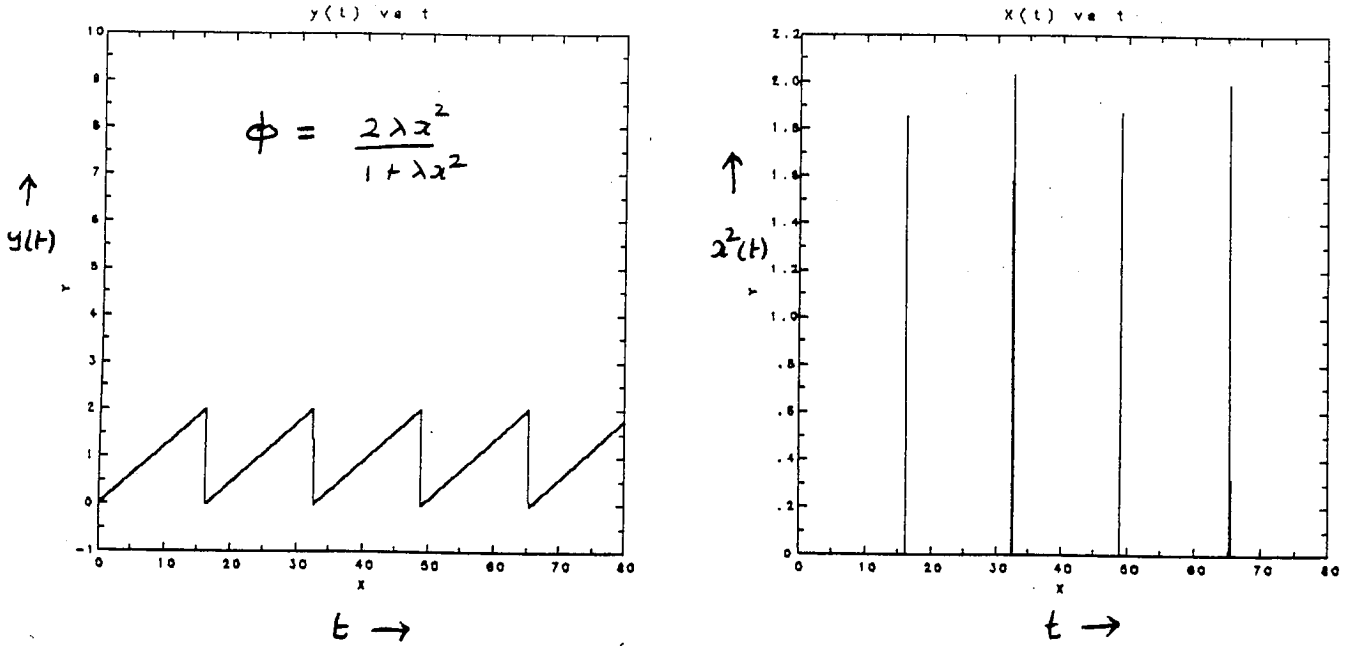


**Fig.4 Extended Model: Unperturbed Solutions**

At this level, the solutions are in fact indistinguishable from those shown in Fig. 1, except for the fact that the maximum of $x^2$ in the two cases is different.

- The fact that the $x^2$ plot shows 'waves' is due to a graphical resolution effect. There are insufficient points within the crash to resolve the wave form properly at the maximum in the *plot* although the simulation itself resolves the crash accurately. This is shown by Fig. 5 which shows the same case but with twice as many frames.

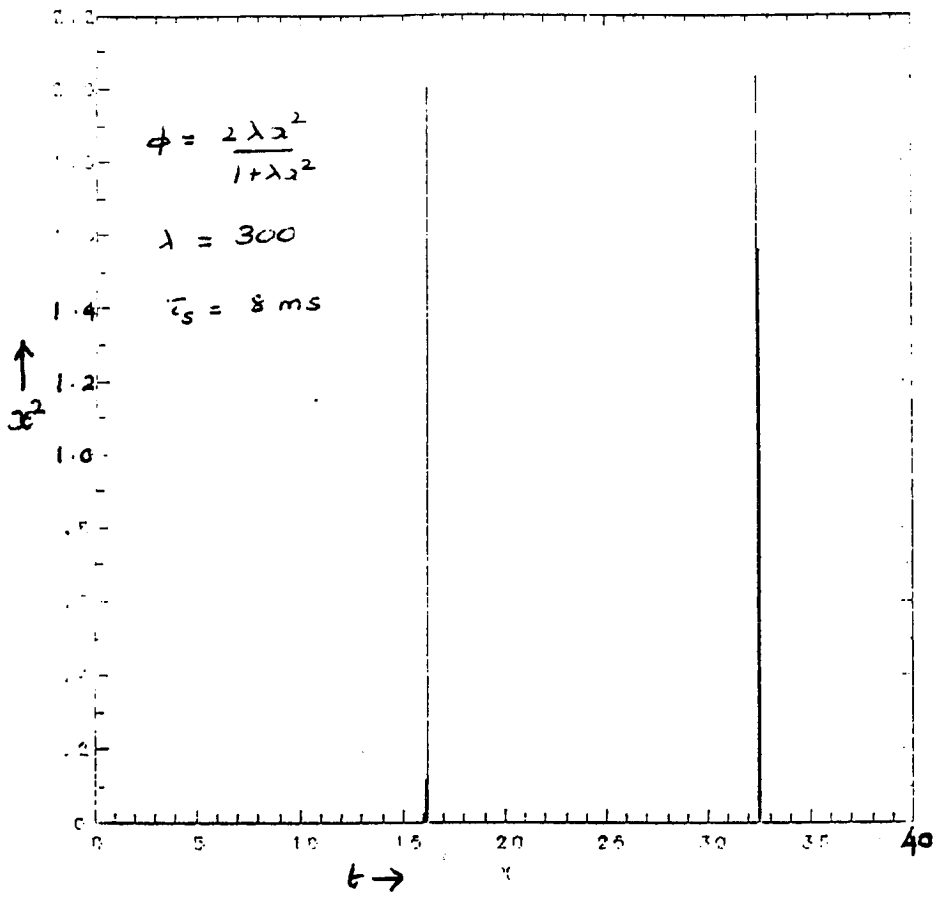


**Fig.5 Extended Model with Increased Plot Resolution**

- We have established that $f_y$ has little or no significant effect

on the extended model, just as in the simple model.

- Fig. 6 presents the solution of the extended model equations for the same conditions as in Fig. 2 except that the value of $f_x$ is deliberately chosen to be twenty times larger.

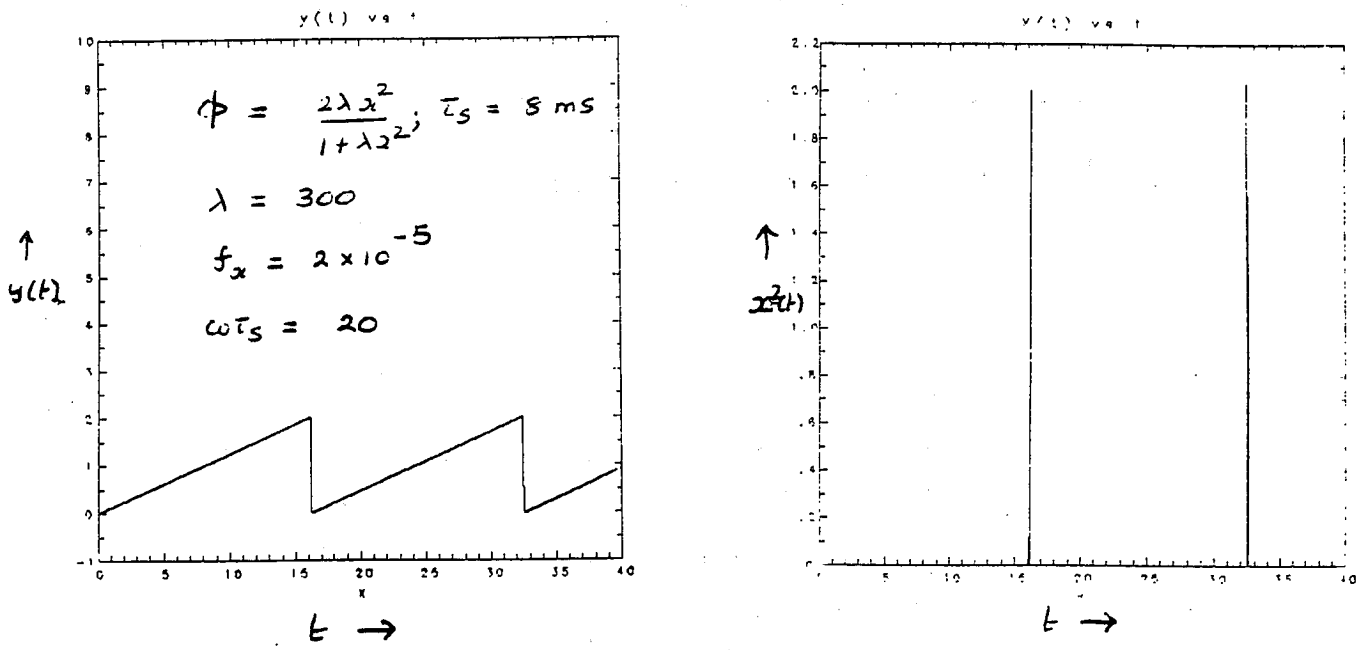


**Fig.6 Effect of Harmonic Perturbation on Extended Model**

We note that in contrast to Fig. 2, the solution is virtually unaffected by the perturbation. This relatively robust behaviour

is typical of the extended model. So long as the external perturbations are such that $\frac{f_x}{\omega\tau_s} \leq x_{min}$, the system appears to be stable both qualitatively and in terms of the numerical values of the period and amplitude.

The following table shows a comparison of the two models. We consider the solutions for the following parameters: $\lambda = 100$, $\omega\tau_s = 200$ (this corresponds to a frequency of 4khz for the external perturbation $f_x$), and $\tau_s = 8$msecs. The values of the reduced period , $T_{red} \equiv \tau_{period}/2\tau_s$ are given for the simple model(I) and for the extended model(II).

| $\frac{f_x}{\omega\tau_s}$ | $T_{red}(I)$ | $T_{red}(II)$ |
|---|---|---|
| $10^{-10}$ | 1 | 1 |
| $10^{-6}$ | 0.9 | 1 |
| $10^{-2}$ | 0.7 | 1 |
| $10^{-1}$ | 1.1 | 1 |
| $10^{-0}$ | No sawteeth | No sawteeth |

- Fig. 7 illustrates the phenomena that occur when the driving force is large amplitude, $\frac{f_x}{\omega \tau_s} = 0.1$ and low frequency, $\omega \tau_s = 2$ in the extended model. Thus, this case is strictly analogous to the 'chaotic' case of Fig. 3. The evidence for partially stabilized sawteeth and period-doubling is apparent.

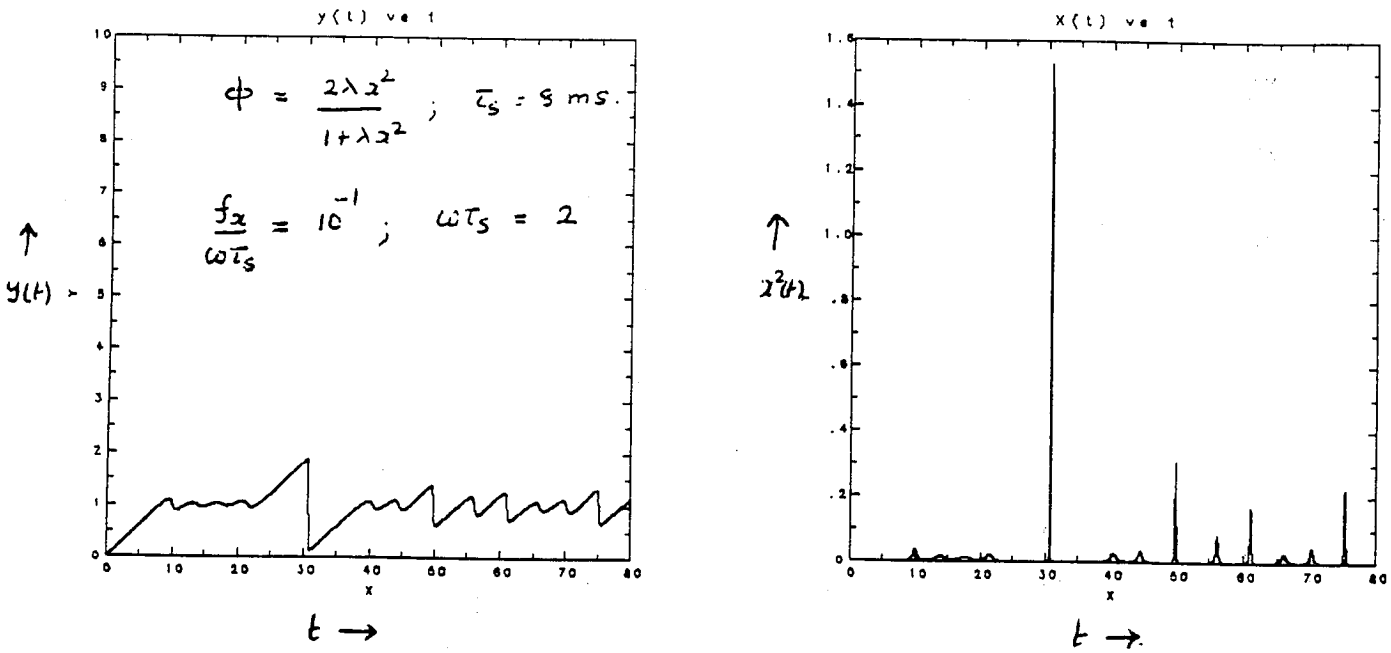


**Fig.7 Extended Model with Large Perturbation**

- We next show a sequence of cases which illustrate the very sharp transition in the nature of the dynamics as $\frac{f_x}{\omega \tau_s}$ is varied in a relatively small range from $\frac{1}{20}$ through $\frac{1}{6}$ keeping $\lambda = 100$, $\omega \tau_s = 200$ $\tau_s = 8$msecs ($\omega$ is equivalent to 4khz). Fig. 8 shows that for $\frac{f_x}{\omega \tau_s} = 0.05$ the solution is nearly identical with the force-free solution (Fig.4).

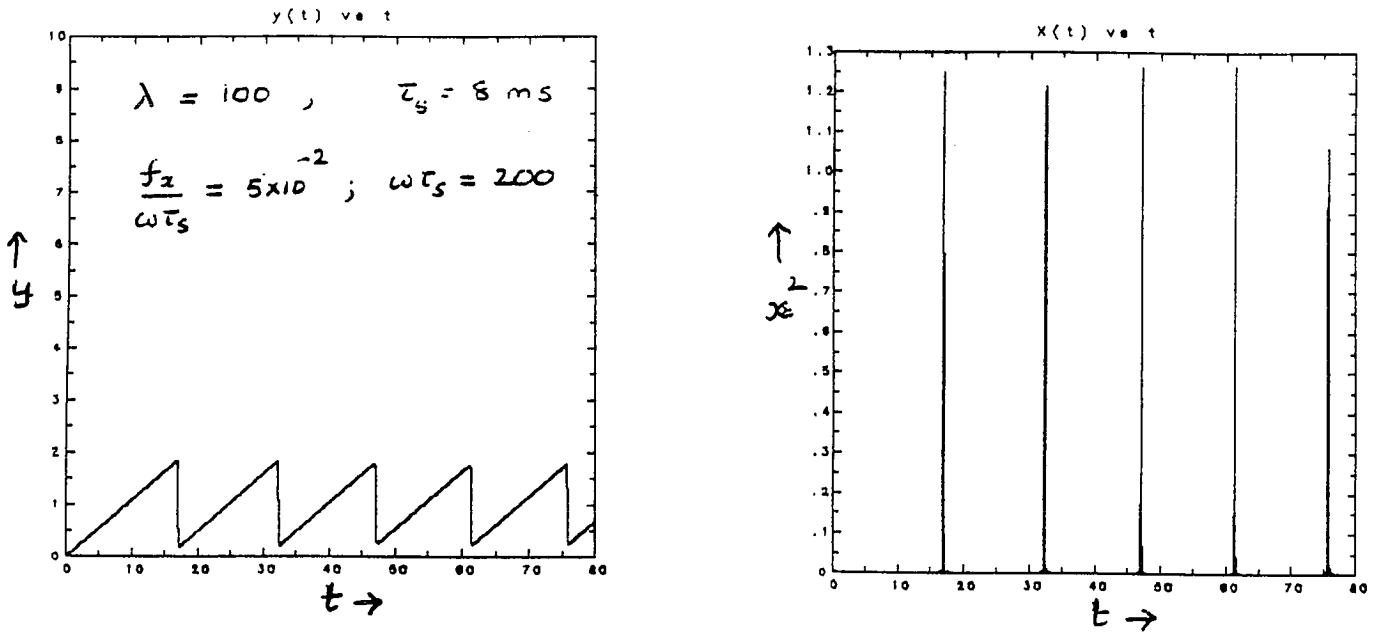


**Fig.8 Extended Model: transition to stability I**

- However, as the amplitude parameter increases through to 0.125, the first crash is postponed to nearly 40 msecs (Fig. 9) and the period increases subsequently by 50%.

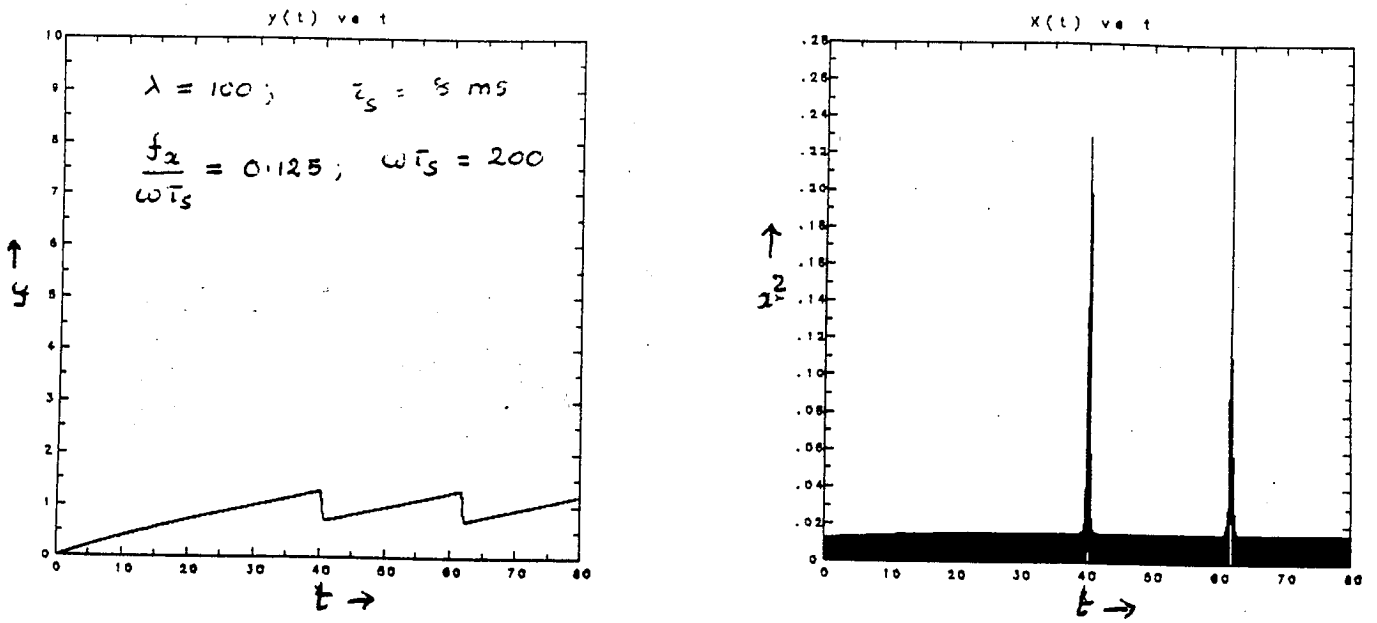


**Fig.9 Extended Model: transition to stability II**

- Fig. 10 illustrates that at a slightly larger amplitude (0.133), the sawtooth is nearly completely stabilized.

$\lambda = 100$ ; $\tau_s = 8$ ms

$\frac{f_x}{\omega \tau_s} = 0.133$ ; $\omega \tau_s = 200$

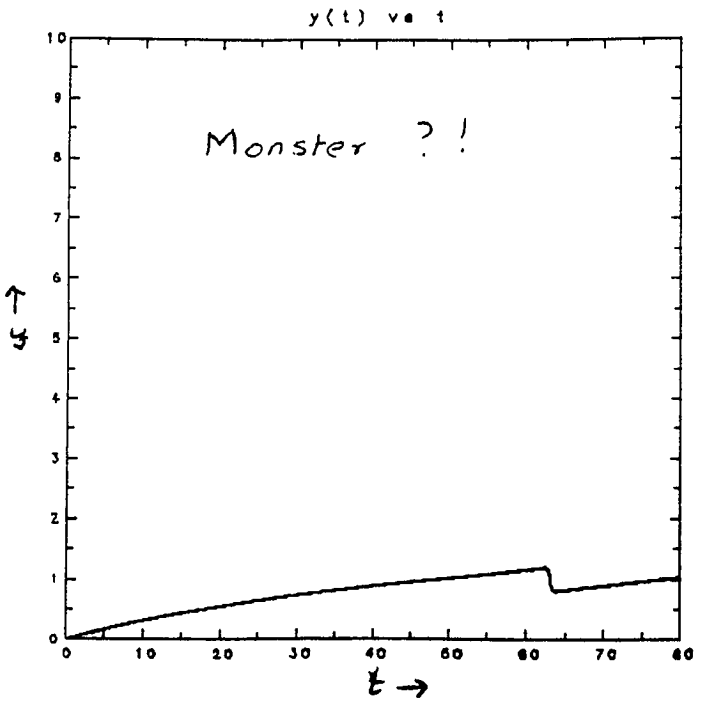


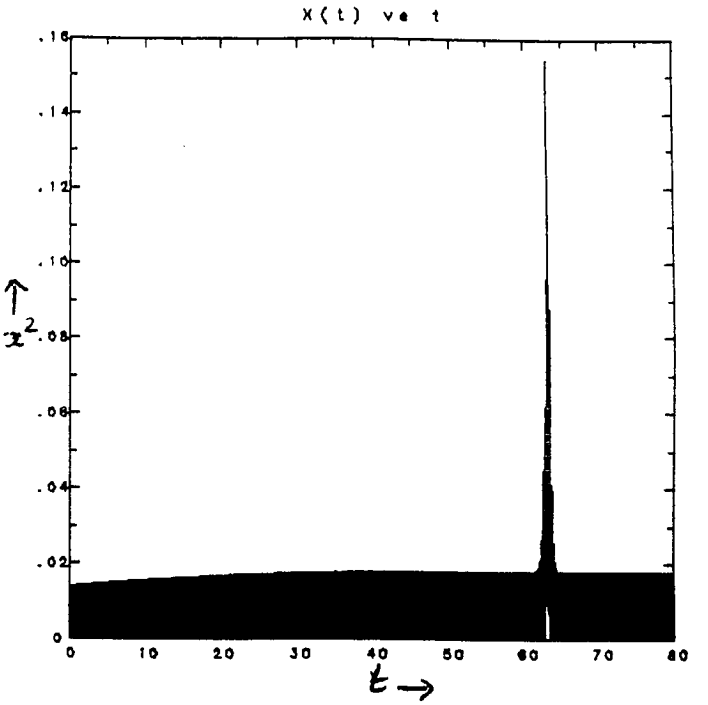


**Fig.10 Extended Model: transition to stability III**

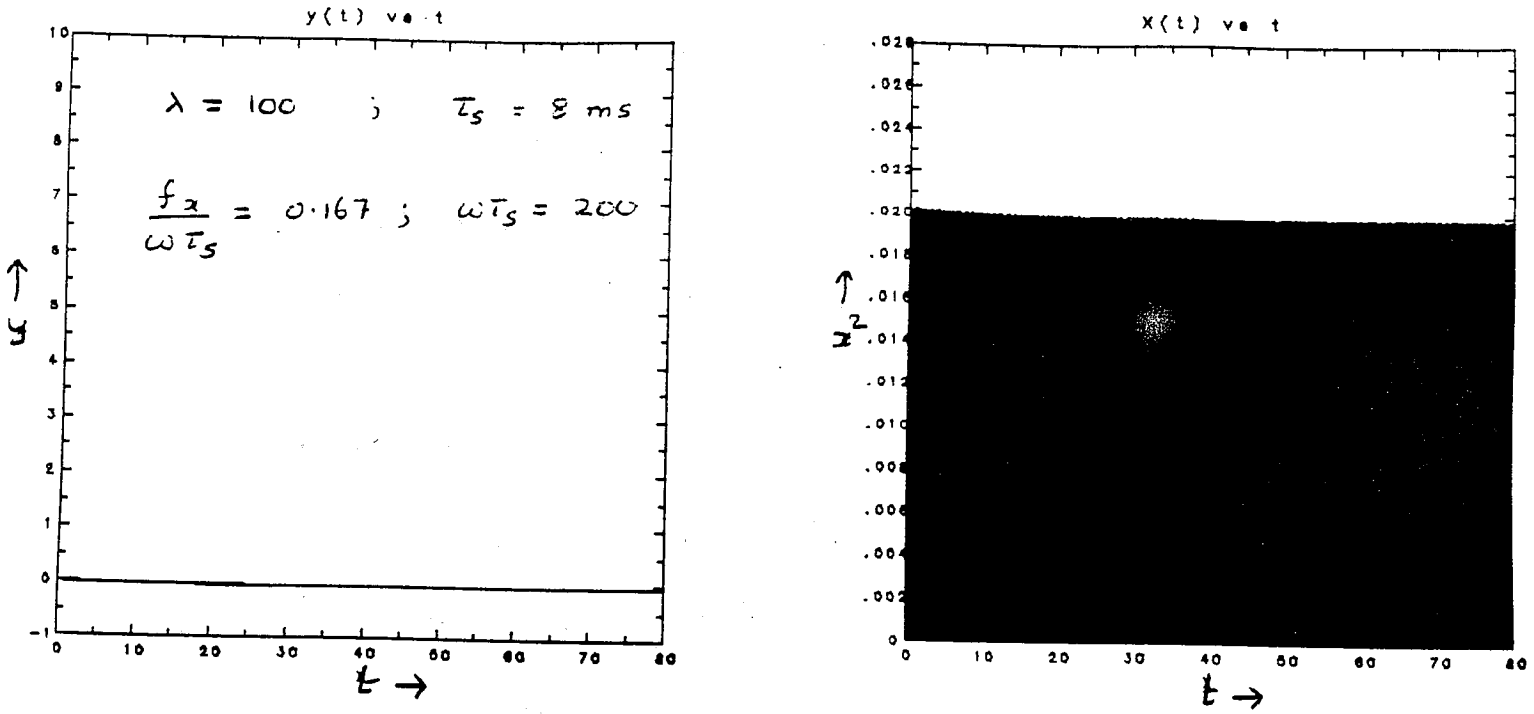


**Fig.11 Extended Model: fully stabilized**

- Fig.11 shows the fully stabilized condition at $\frac{f_x}{\omega \tau_s} = 0.167$. It is easily seen from the equations that $< x^2 >= \frac{1}{\lambda}$ and $< y(t) >= 1$. If the external force is stronger, the saturation value of $< y >$ decreases to compensate for the extra driving.

## VII. Discussion and Conclusions

- Very simple dynamic models have been constructed and shown to be capable of reproducing important aspects of sawteeth in tokamaks as regards temporal behaviour. These models bear the same relation to more sophisticated physical treatments of sawtooth phenomena using partial differential equations or kinetic equations which the Lorenz model has to the fluid equations of convective heat transfer.

- The purpose of the models is to understand in a very simplified manner the possible relationship between transport processes and sawtooth dynamics. While there is no derivation as yet in detail of the models from more complete physical equations such as the resistive MHD reduced equations, the periodic character of sawteeth suggests that a two-degree of freedom dynamic system such as those obtained here is probably involved in the gross temporal phenomena associated with them.

- Fig. 12 is taken from a typical simulation by Aydemir (private communication, 1991). It shows the behaviour of the

magnetic field energy in the higher $m \simeq n$ components. The resemblance of the wave form to that of the $x^2$ variable is indicative that the identification of $x(t)$ as a measure of turbulence amplitude may be physically reasonable.

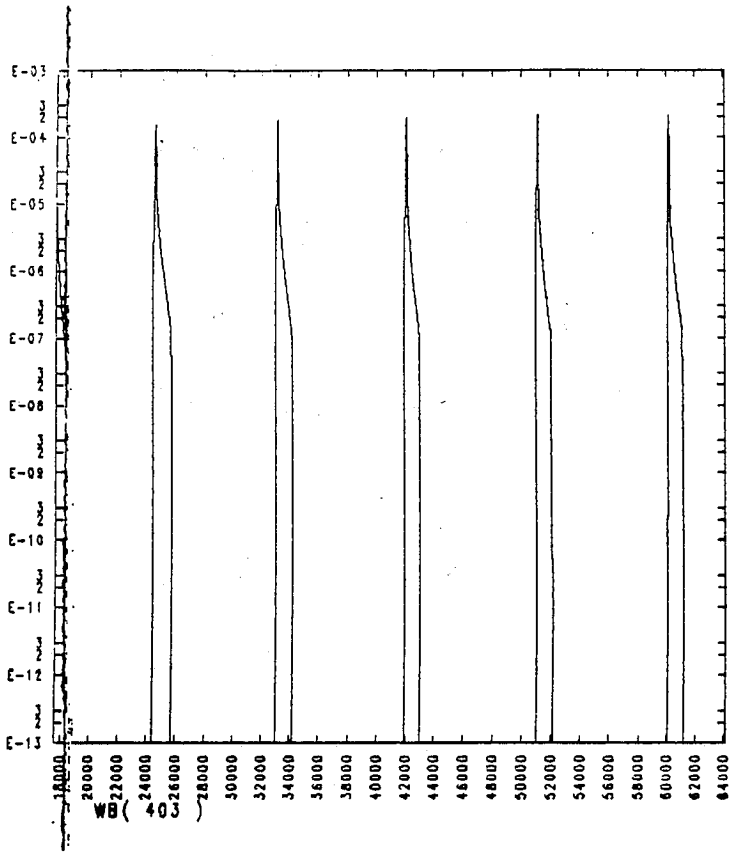


**Fig.12 RMHD Calculation of Magnetic Turbulence Energy**

- The extended model shows that the sawtooth oscillation need not necessarily involve simple linear instabilities but essentially *nonlinear* damping and growth of turbulence as the temperature (or internal energy) of the plasma varies on the ramp time-scale. Furthermore, the turbulence amplitudes will not (unlike the simple model) reach unphysically small amplitudes during the ramp phase. The growth rate of the turbulence at the maximum is determined by the parameter $\lambda$ which is simply related to the ratio of the period and crash time-scales. The inverse of this parameter is related to the level of turbulence during the ramp during which the latter grows on the time-scale $\tau_s$ rather than the much shorter crash timescale. The $\phi$ term essentially acts as a nonlinear 'brake' on the steadily growing *linear* growth rate, $\frac{\lambda}{\tau_s}(y(t)-1)$ during most of the ramp.

- The realistic model is indeed robust to both coherent and incoherent perturbations for reasonably small amplitudes.

- However, the simulations show that harmonic perturbations of appropriate frequency and amplitude could lead to partial

and total stabilisation of sawteeth. This result could have considerable practical significance in the control by external means of sawtooth and other gross instabilities if it is extended to physically-based dynamic models.

- Indeed, it is possible that certain observations in TEXT (S.McCool, private communication, 1991) where sawteeth are known to be absent in the presence of a large MHD mode (typically $m = 2$) even when a finite $q = 1$ radius is indicated (in pellet data) could be explained qualitatively with our model.

- Thus Fig.13 shows the brightness dip at the $q = 1$ surface in shot # 161575 in TEXT ($B_{tor} = 20$ kgauss, $I_p = 171$ kAmps, $\bar{n_e} = 1.8 \times 10^{13}$ /cc; strong $m = 2$ and a carbon pellet), when there is no sawtooth activity, which is presumed to have been suppressed by the MHD.

- Fig.14 shows a different diagnostic (SXR and Mirnov coils) producing an equivalent result (also in TEXT) . In shot # 139071, it is evident that while the strong MHD oscillation (lower trace) is on, the sawteeth are suppressed (upper trace).

The latter comes on a 10 msec time-scale with an estimated inversion radius of 6.2 cm ($r_{q=1} \simeq 7$ cm). Since the resistive time-scale is of order 70 msec, this is suggestive evidence for m=2 stablilisation of sawteeth.

- Research is being directed at present to derive the model from physics-based equations of motion. Such a derivation would throw light on the physical processes that are responsible for $\lambda$ and $\tau_s$ and also fix the correct normalisations of $y(t)$ and $x(t)$ in terms of experimentally determinable quantities.

- Finally, it is of interest to show that these models are actually particular cases of a more general class of equations having a structure similar to those which might be expected from a complete spectral representation of the full non-linear equations governing sawteeth in tokamaks.

  Thus consider a set of M "amplitude" functions (M need not necessarily be finite), $x_i(t)$, $i = 1, 2, .., M$. Let these functions satisfy the following system of M non-linear, coupled

equations:

$$\frac{dx_i}{dt} = \frac{\lambda}{\tau_s}(Y-1)x_i + \sum_{j=1}^{M} T_{ij}x_j, \qquad (26)$$

where, the interaction matrix $T_{ij}$ is merely required to be anti-symmetric in its suffixes, but may otherwise be an entirely arbitrary function of t, Y, and the variables $x_i$ themselves. The dynamical evolution of these amplitudes can be extremely complicated and indeed chaotic in general. Yet, it is easy to see that $X(t) = \sum_{i=1}^{i=M} x_i^2(t)$ actually satisfies the simple model equations. A similar result also applies to the extended model. This example suggests (but of course does not prove) how the complete set of evolution equations for a tokamak plasma could contain simple sawtooth behaviour within them in the sense of reducing to the model constructed.

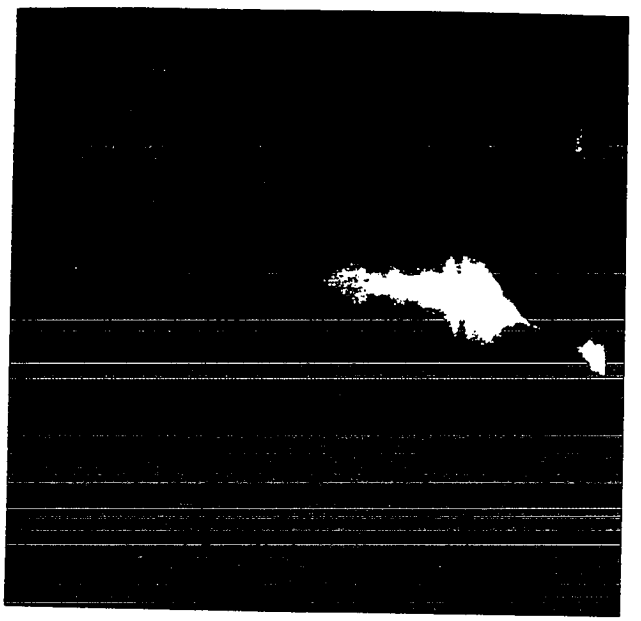

**Fig.13 Evidence from TEXT of q=1 Surface with Strong MHD but no Sawtooth Activity: shot No. 161575**

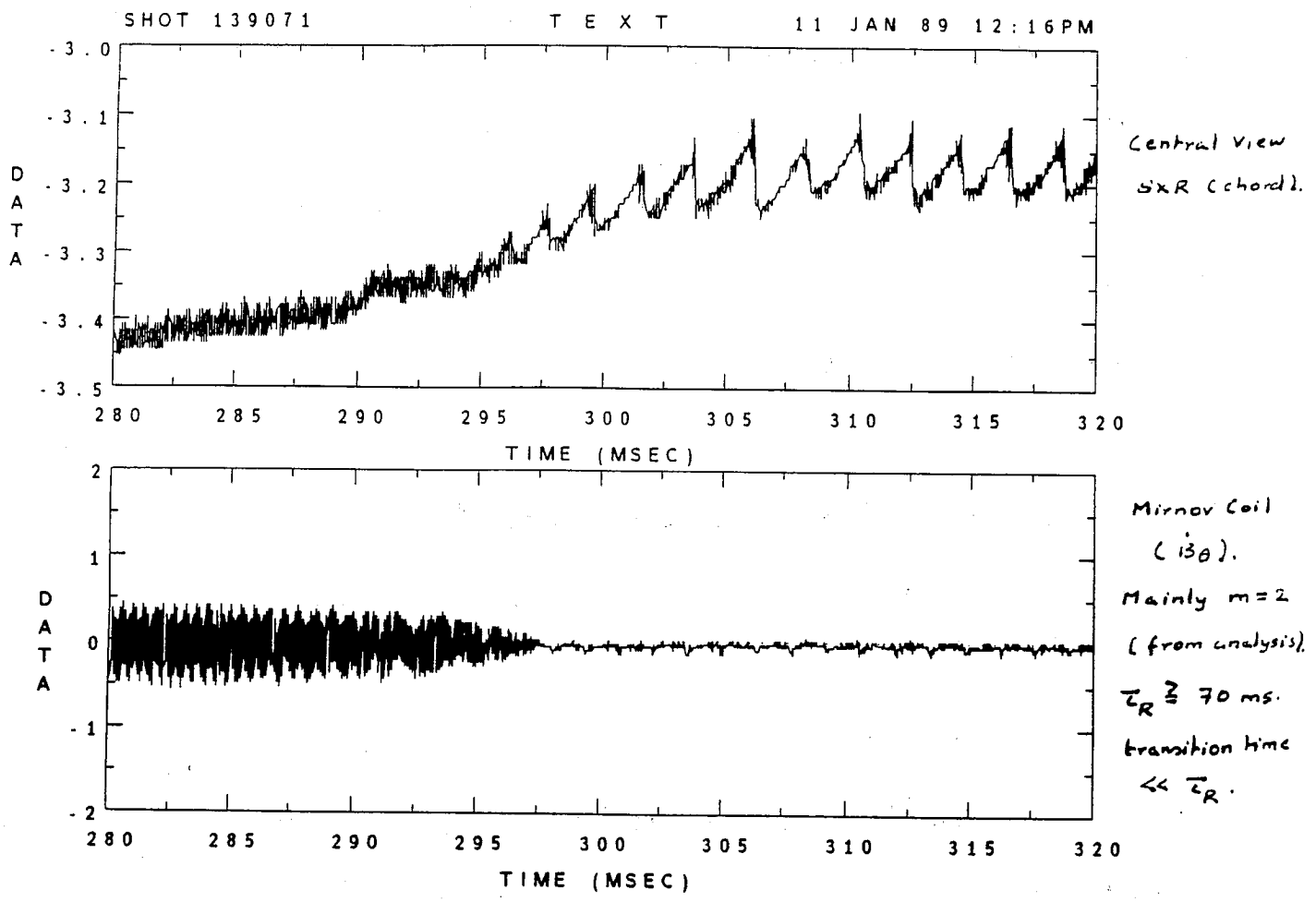


**Fig.14 Evidence from TEXT of MHD-Sawtooth complementarity**

## References

[1]A.Y. Aydemir, J.C. Wiley, and D.W. Ross, Phys. Fluids **B** 1, 774, (1989).

[2]R.E. Denton, J.F. Drake, R.G. Kleva, and D.A. Boyd, Phys. Rev. Letts. **56**, 2477, (1986).

[3]F.A. Haas and A. Thyagaraja, AEA Fusion Report, AEA FUS 87, Culham Lab. (1990).

[4]E.T. Whittaker and G.N. Watson, *A Course of Modern Analysis*, (Cambridge Univ. Press, New York, 1980), Chs. 11,12.

**Acknowledgements:**

One of us (AT) thanks Prof. Baldwin for his hospitality during his visit to the IFS. We also gratefully acknowledge stimulating discussions with A.Y Aydemir, G.G. Castle, W.A. Craven, S.C. McCool and R.D. Hazeltine. In particular thanks are due to Drs. Aydemir and McCool for permission to present Figs. 12, 13 and 14 in the present work.